Atmospheric Environment 66 (2013) 52–62

Contents lists available at SciVerse ScienceDirect

Atmospheric Environment

journal homepage: www.elsevier.com/locate/atmosenv

Effects of soil moisture on the diurnal pattern of pesticide emission: Comparison of simulations with field measurements

Rivka Reichman [a,*], Scott R. Yates [a], Todd H. Skaggs [a], Dennis E. Rolston [b]

[a] U.S. Salinity Laboratory, USDA-ARS, 450 W. Big Springs Rd., Riverside, CA 92507, USA
[b] Land, Air and Water Resources, University of California, One Shield, Ave., Davis, CA 95616, USA

HIGHLIGHTS

- We investigate soil moisture effects on diazinon volatilization from soil.
- Volatilization is simulated with a comprehensive non-isothermal model.
- Simulated volatilization rates are compared with measured values.
- Soil-water content strongly affects the magnitude and timing of volatilization.
- Soil-water content impacts volatilization because of its effect on vapor sorption.

ARTICLE INFO

Article history:
Received 10 November 2011
Received in revised form
19 April 2012
Accepted 24 April 2012

Keywords:
Model validation
Volatilization rates
Diazinon
Soil moisture effect

ABSTRACT

Pesticide volatilization from agricultural soils is one of the main pathways in which pesticides are dispersed in the environment and affects ecosystems including human welfare. Thus, it is necessary to have accurate knowledge of the various physical and chemical mechanisms that affect volatilization rates from field soils. A verification of the influence of soil moisture modeling on the simulated volatilization rate, soil temperature and soil-water content is presented. Model simulations are compared with data collected in a field study that measured the effect of soil moisture on diazinon volatilization. These data included diurnal changes in volatilization rate, soil-water content, and soil temperature measured at two depths. The simulations were performed using a comprehensive non-isothermal model, two water retention functions, and two soil surface resistance functions, resulting in four tested models. Results show that the degree of similarity between volatilization curves simulated using the four models depended on the initial water content. Under fairly wet conditions, the simulated curves mainly differ in the magnitude of their deviation from the measured values. However, under intermediate and low moisture conditions, the simulated curves also differed in their pattern (shape). The model prediction accuracy depended on soil moisture. Under normal practices, where initial soil moisture is about field capacity or higher, a combination of Brooks and Corey water retention and the van de Grind and Owe soil surface resistance functions led to the most accurate predictions. However, under extremely dry conditions, when soil-water content in the top 1 cm is below the volumetric threshold value, the use of a full-range water retention function increased prediction accuracy. The different models did not affect the soil temperature predictions, and had a minor effect on the predicted soil-water content of Yolo silty clay soil.

Published by Elsevier Ltd.

1. Introduction

Pesticide volatilization from agricultural soils is one of the main pathways in which pesticides are dispersed in the environment (Taylor and Spencer, 1990; Glotfelty et al., 1984; Wang et al., 1997). To better protect agricultural workers and surrounding communities from potentially toxic emissions, it is necessary to have accurate knowledge of the various physical and chemical mechanisms that affect volatilization rates from field soils.

Pesticide volatilization rates are known to exhibit diurnal fluctuations. The magnitude and timing of the fluctuations depend on the moisture content of the soil surface. When the surface is relatively wet, the fluctuations coincide with diurnal variations in solar radiation or surface soil temperature, such that pesticide emissions typically achieve a maximum in the early afternoon and

* Corresponding author. Environmental Physics Dep., Israel Institute for Biological Research, P.O. Box 19, Ness-Ziona 74100, Israel.
E-mail address: rikir@iibr.gov.il (R. Reichman).

1352-2310/$ – see front matter Published by Elsevier Ltd.
doi:10.1016/j.atmosenv.2012.04.047

a minimum at night. But if the surface dries sufficiently, the pattern is different, with peak volatilization rates typically occurring in the early morning (Glotfelty et al., 1989; Prueger et al., 2005; Gish et al., 2009; Reichman et al., 2011).

A variety of emission models with varying levels of complexity have been developed to calculate hourly emission rates (Baker et al., 1996; Wang et al., 1997, 1998; Reichman et al., 2000; Scholtz et al., 2002a; Yates, 2006; Bedos et al., 2009), which are important for determining the risks of acute inhalation toxicity. Comparisons of model predictions with field measurements have often found the predicted magnitude of the volatilization flux to be in good agreement with data, although the timing of the maximum flux rate is often poorly predicted (Baker et al., 1996; Scholtz et al., 2002b; Bedos et al., 2009). Accurate prediction of the timing of diurnal of the diurnal fluctuations requires knowledge of the surface soil moisture content. When the water content drops below a critical value, soil particles are no longer completely covered by liquid water, pesticide vapor pressure (Spencer et al., 1969) and consequently emissions (Spencer and Cliath, 1973) drop to very low values due to pesticide vapor sorption to the exposed particle surfaces. Soil-water content effects are especially important in adsorption of relatively nonpolar organic chemicals by soil (Spencer et al., 1982).

Reichman et al. (submitted for publication) described a comprehensive non-isothermal simulation model and evaluated the sensitivity of various model parameters and components in predicting surface soil-water content and pesticide emissions. Simulations of diazinon (O, O diethyl O-(2-isopropyl-4-methyl-6-pyrimidinyl) phosphorothioate) volatilization were performed over ten days of drying in loam and sand soils. The analysis included sensitivity calculations for the soil air–solid interface partition coefficient (K_g), as well as an assessment of differing possible parametric representations for the soil-water retention (WR) function and the soil surface resistance (SSR) term. Reichman et al. (submitted for publication) found that the temporal variation and magnitude of diazinon emission are strongly affected by the value of K_g. The SSR functions affect volatilization rates due to their effect on soil-water content. The WR functions had a relatively minor effect on both the simulated water content and volatilization rates. The simulated soil temperature was not affected by the choice of WR and SSR functions.

The purpose of the present study was to verify the influence of soil moisture modeling on the simulated volatilization rate, soil temperature and soil-water content. The current paper builds on the work of Reichman et al. (submitted for publication) by comparing simulations of diazinon volatilization with data taken from a field study that measured emissions under varying soil moisture conditions (Reichman et al., 2011). These data include diurnal changes in volatilization rates, near-surface soil-water contents, and soil temperatures.

2. Materials and methods

2.1. Field experiments

The measured data used in the present research were collected in a field study comprising three experiments performed with differing soil moisture conditions. The duration of each experiment was three days. A complete description of the experimental methods is given in Reichman et al. (2011). The field site was located at a research facility of the University of California at Davis. The soil was Yolo silt loam (fine-silty, mixed, non-acid, thermic Typic Xerorthent) consisting of 35% sand, 47% silt, 18% clay and 1.48% organic matter content. Volatilization rates were measured using flux chambers (Reichman and Rolston, 2002). Three field plots measuring 2 m × 1.2 m were used for the different experimental treatments. Each plot contained two chamber bases (40 cm × 40 cm × 6 cm) that served as two replications (identified as Loc1 and Loc2). The chamber bases were inserted 6 cm into the soil. Volatilization rates were measured by alternating the placement of the flux chamber onto one of the two chamber bases. Diazinon was applied to the bare soil surface by hand spraying at a rate of 1–1.5 kg ha^{-1}. The applications were at 10 AM, 9 AM and 8:30 AM for experiments 1, 2 and 3, respectively. The initial volumetric water contents in the surface layer (0–1 cm) were 0.22, 0.075 and 0.29 cm^3 cm^{-3} for experiments 1, 2 and 3, respectively. In experiment 3, 1 mm of water was applied 1 h after spraying. The initial water contents were determined gravimetrically from soil samples collected from the field plot outside the chamber bases.

The diurnal variation of soil moisture and temperature was measured at 2 soil depths, 1 and 5 cm. The diurnal variations of soil moisture were measured using Time Domain Reflectometry (TDR). At the end of the experiments, soil samples from the 0–2 cm and 4–6 cm soil layers within the chamber frames were taken for determination of bulk density and gravimetric moisture. Variations of the meteorological parameters solar radiation, wind speed, air temperature, and humidity were measured 2 m above ground using a standard meteorological station placed near the site.

2.2. Numerical simulations

The numerical simulations were performed with a comprehensive non-isothermal model (Reichman et al., 2000, submitted for publication). The model describes one dimensional transport of heat, water (liquid and vapor), and chemicals (solute and vapor) in the soil-atmosphere continuum under diurnal variation of atmospheric parameters. The model assumes that contaminant resides in the soil pores as vapor and liquid and can be adsorbed, from both phases, to the soil particles. The partition coefficients between the three phases depend on temperature, soil-water content, and soil constituents.

In the model calculations, two WR functions and two SSR functions were considered. The WR functions evaluated were the Brooks and Corey (1964) (BC) relationship and the full-range WR function proposed by Silva and Grifoll (2007) (SG). The latter aims to improve modeling of soil-water content in the dry region by dividing the retention function, θ (Ψ), into three regions: the capillary region ($\Psi > -1.5 \times 10^4$ cm) where the BC model is used, the adsorptive region (-1.5×10^4 cm $> \Psi > -1.6 \times 10^6$ cm) where the Bradley adsorption isotherm is used, and the hyper-adsorptive region ($\Psi > -1.6 \times 10^6$ cm) where the Brunauer–Emmett–Teller (BET) adsorption isotherm is used. The SSR approach to modeling evaporation augments the usual non-isothermal water transport formulation with a function that introduces additional resistance to vapor flow as the surface dries out and the evaporation front moves below the soil surface. The two SSR approaches examined in the present work are the β wetness function proposed by Deardorff (1978) (D) and the resistance function proposed by van de Griend and Owe (1994) (VDG). The two WR models and two SSR models permit the following WR × SSR combinations: BC–D, BC–VDG, SG–D and SG–VDG. A complete description of these models is given in Reichman et al. (submitted for publication).

To simulate the effect of the flux chamber on the environmental conditions (soil temperature and soil-water content) and diazinon volatilization rates, the following modifications were introduced. A new input data file containing the sampling times was created for the two locations in each of the three experiments. During the sampling time, the short (solar) and long wave radiations were modified to account for the presence of the chamber. The expression for the solar radiation was multiplied by a new parameter taking the value 1 for open atmosphere and 0 for covered

headspace. The long wave radiation incoming from the covered headspace (R_L) was calculated using the Stefan–Boltzman equation

$$R_L = \varepsilon\sigma T^4 \quad (1)$$

where ε and T are the emissivity and the temperature of the enclosed headspace air, respectively, and σ is the Stefan–Boltzmann constant. In the present study we took $\varepsilon = 1$, assuming that the galvanized metal of the chamber behaves as a black body. A black body is a hypothetical object that absorbs all incident electromagnetic radiation while maintaining thermal equilibrium. No light is reflected from or passes through a black body, but radiation is emitted. At room temperature, no visible light is emitted from black body. No physical object exactly fits this definition, but most behave at least in part as black bodies (Reif, 1976). The enclosed air temperature and relative humidity were assumed to be the same as ambient air temperature and relative humidity.

The transfer coefficient between the air and soil surface, h_c, during sampling was modified to:

$$\begin{aligned} h_c &= 0.21^*(T_{z=0} - T)^{0.25} \quad T_{z=0} > T \\ h_c &= 0.11^*(T_{z=0} - T)^{0.25} \quad T_{z=0} < T \end{aligned} \quad (2)$$

where $T_{z=0}$ is the soil surface temperature. This transfer coefficient, defined for heat convection between a horizontal surface and the air above it at atmospheric pressure, has previously been applied to heat convection in greenhouses (Avissar and Mahrer, 1982; Kimball, 1973).

Diazinon and soil properties used for the simulations are given in Tables 1 and 2, respectively. The variations of the meteorological parameters (solar radiation, air temperature, air relative humidity and wind speed) measured during experiments 1, 2, and 3 are given in Fig. 1.

2.3. Statistical analysis

The evaluation of the models included comparisons between measured and predicted values of temporal variations of soil temperature, soil-water content and diazinon volatilization rate. Quantitative comparisons included residual error analysis and graphical display, and assessments of accuracy and precision. Accuracy is the extent to which the predicted values approach a corresponding set of measurements. Precision is the degree to which predicted values approach a linear function of measured observations.

Three goodness-of-fit measures were used for residual error analysis: Root Mean Square Error (RMSE), Normalized Root Mean Square Error (NRMSE) and bias. For a model that accurately predicts the measured values, the RMSE, NRMSE and bias should have values close to 0. RMSE and NRMSE were used to evaluate which of the model formulations provided the best overall agreement with the measured data. The bias was used to evaluate model overestimation (positive bias) or underestimation (negative bias). The expressions used to calculate RMSE, NRMSE and bias are,

$$\mathrm{RMSE} = \sqrt{\frac{1}{n}\sum_{i=1}^{n} d_i^2} \quad (3)$$

$$\mathrm{NRMSE} = \mathrm{RMSE} \times 100/\overline{M} \quad (4)$$

$$\mathrm{bias} = \frac{1}{n}\sum_{i=1}^{n} d_i \quad (5)$$

where d_i is the deviation between model and prediction, n is the number of observations and $\overline{M}$ is the mean of measured data. For soil temperature and soil-water content, d_i was defined as, $d_i = P_i - M_i$, where P_i is the predicted value, M_i is the measured value, and for the volatilization rates it was defined as, $d_i = \log(P_i) - \log(M_i)$. For these definitions, the dimensions for d_i for soil temperature and soil-water content are °C and $cm^3\ cm^{-3}$, respectively, and d_i is dimensionless for the volatilization rates.

Table 1
Diazinon properties used for simulation.

Property	Value
Molecular weight	304 g mol^{-1}
Water solubility	40 ppm
Air diffusion coefficient[a]	174 $cm^2\ h^{-1}$
Water diffusion coefficient[b]	0.015 $cm^2\ h^{-1}$
Degradation coefficient[c]	0.03 d^{-1}
Sorption coefficient	
Soil-water–organic matter partitioning coefficient (K_{om})[d]	1520 $cm^3\ g^{-1}$OM
Soil air–solid interface partitioning coefficient (K_g)[e]	11,050 $m^3\ g^{-1}$
Fitting parameters for $x(\theta_g)$[f]	
ξ	12.1
ζ	104.4
Vapor pressure-temperature relation[g]	Log P (mmHg) = 9.3871 − 4014.67/T (K)

[a] The diazinon diffusion coefficient in air was calculated using the Fuller et al. (1966) expression.
[b] The diazinon diffusion coefficient in water was taken from Lin et al. (1996).
[c] Loam soil (pH = 4.8, 20 − 30 °C). From Bro-Rasmussen et al. (1970).
[d] Based on $K_d = 22.87\ cm^3\ g^{-1}$ measured for Yolo silt loam soil that contains 1.5% organic matter (Chen et al., 2000).
[e] Based on measurement of diazinon vapor adsorption to Yolo silt loam (Chen et al., 2000).
[f] Measured and fitted for Yolo silt loam (Chen et al., 2000).
[g] The vapor pressure dependence on temperature was taken from Kim et al. (1984), who measured it using the gas saturation method.

Table 2
Soil properties used for simulations.

Property	Value
Soil physical properties	
Sand/silt/clay	22/56/22 (%)
Bulk density	1.13 g cm^{-3} (exprt#1); 1.2 g cm^{-3} (exprt#2); 1.35 g cm^{-3} (exprt#3)
Porosity	0.495
Hydraulic properties	
K_{hs}	0.1 cm d^{-1}
m	6.45
ϕ	0.2
ψ_{cr}	−46.4 cm
θ_s	0.495 $cm^3\ cm^{-3}$
θ_r	0.01 $cm^3\ cm^{-3}$
θ_{fc}	0.3 $cm^3\ cm^{-3}$
θ_{min}	15%
Water adsorption isotherm[a]	
BET isotherm parameters	
B	128.07
W_m	15 mg g^{-1}
Bradely isotherm parameters	
a	15.35
b	−36.76
Photometric properties	
Short wave radiation	
Albedo	0.2
Absorption	0.8
Long wave radiation	
Reflectivity	0.1
Absorption	0.9
Emissivity	0.9

[a] Chen et al. (2000).

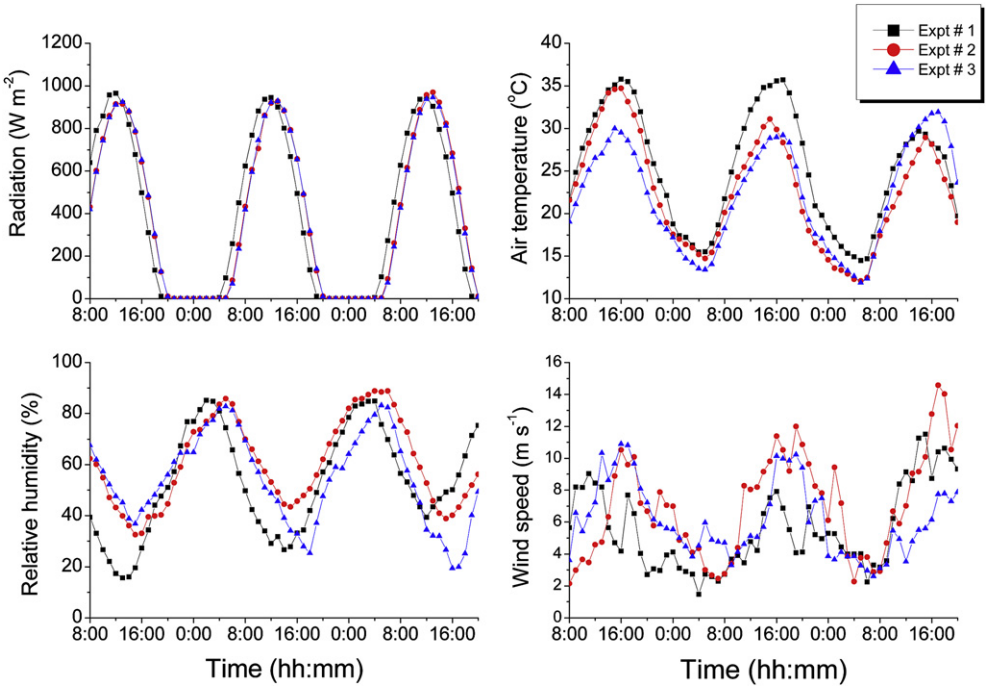

Fig. 1. The diurnal variation of the meteorological parameters used as input for simulation.

The graphical display analyses included scatter plots of predicted vs. measured values and a linear regression of these values. A simulation that predicts the measured values precisely would have a regression line with a slope, intercept and R^2, respectively, of 1, 0, and 1.

3. Results and discussion

3.1. Soil temperature

Typical diurnal variations of measured and simulated soil temperatures at 1.5 and 5 cm are presented in Fig. 2. These data are from Experiment 3 (the wettest initial soil conditions) at Loc 2. Goodness-of-fit measures for the soil temperature in all three experiments are given in Table 3, and scatter plots are shown in Fig. 3.

Model predictions for soil temperature made using the different WR × SSR combinations were all very similar (Reichman et al., submitted for publication). In general, the predicted soil temperatures were in good agreement with observations (Fig. 2). The RMSE ranged from 1.4 to 3.6 °C, the NRMSE from 4 to 12%, and the maximum bias was about 2 °C (Table 3). Similar RMSE and NRMSE values were obtained for Experiments 1 and 3, whereas higher values were obtained for Experiment 2 (drier soil). This result indicates that the prediction of soil temperature under wet conditions was more accurate. On average, the various model formulations all underestimated soil temperature at 1.5 cm and overestimated it at 5 cm when there was relatively wet conditions (Experiments 1 and 3), whereas they overestimated the temperature at both depths under drier conditions (Experiment 2). The underestimated soil temperature under wet conditions was likely caused by higher heat capacity under wet conditions than dry. Linear regression between predicted and measured values resulted in slope values between 0.98 and 1.16, intercept values between −3.59 and 1.04, and R^2 values between 0.91 and 0.94 (Fig. 3). Linear regression performed for individual experimental trials resulted in values of R^2 ranging between 0.93 and 0.99 (Table 3), indicating a high level of precision for temperature predictions.

3.2. Soil-water content

Typical diurnal variations of measured and simulated soil-water content at 1.5 and 5 cm are presented in Fig. 4. These data were obtained for Experiment 3 (the wettest soil) at Loc 2. A summary of the statistical analysis for the three experiments and two soil depths is given in Table 4, and scatter graphs are shown in Fig. 5. In general, Reichman et al. (2011) found that their TDR measurements were in good agreement with the gravimetrically determined soil-water contents except the measurements in Experiment 2 at 1.5 cm. Consequently, those TDR data were omitted from the statistical analysis (Table 4). Temperature effect on TDR reading was neglected as the volumetric soil-water content was less than 0.3, a threshold value that above which a noticeable effect was observed (Gong et al., 2003).

The four model configurations predicted very similar soil-water contents for the two soil depths. The predicted values for soil-water content underestimated observations during the first two days at 1.5 cm and overestimated them during the first 8 h at 5 cm. For rest of the time, a good agreement with observations was observed (Fig. 4). The RMSE values ranged from 0.018 to 0.062 $cm^3\ cm^{-3}$, NRMSE values from 9 to 33%, and the maximum bias was about 0.056 $cm^3\ cm^{-3}$ (Table 4). Better goodness-of-fit values were obtained at 5 cm, indicating that soil-water prediction at the deeper depth was more accurate. Linear regression between predicted and measured values at 1.5 cm resulted in values for the slope between 0.39 and 0.62, for the intercept between 0.02 and 0.07, and for R^2 between 0.76 and 0.80 (Fig. 5 and Table 4). At 5 cm, the linear regression resulted in values for the slope between 0.74 and 0.83, for the intercept between 0.04 and 0.06, and for R^2 between 0.23 and 0.30 (Fig. 5 and Table 4). These results show that the precision of predicted soil-water content is lower than the precision of the predicted soil temperature (Fig. 3).

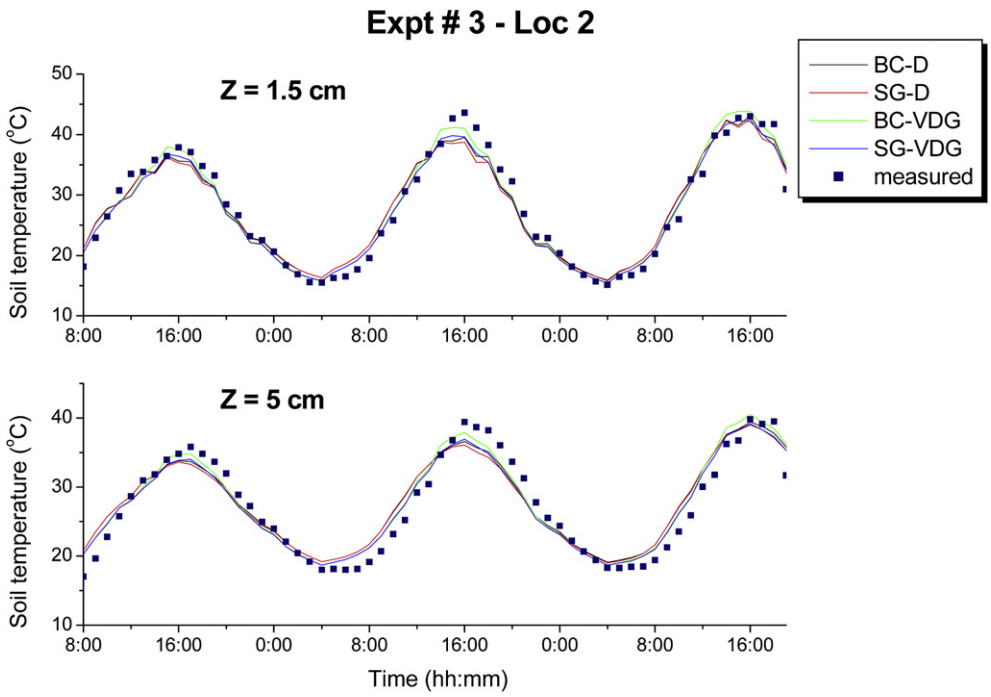

Fig. 2. Temporal variation of measured and simulated soil temerature at two depths (about 1.5 and 5 cm) during the three days of Experiment 3 (Loc 2). (BC = Brooks–Corey water retention function; SG = Silva and Grifoll (2007) full-range water retention model; D = the β wetness surface resistance function of Deardorff (1978); VDG = the surface resistance function proposed by van de Griend and Owe (1994)).

3.3. Volatilization rates

The diurnal variation of measured and simulated volatilization fluxes for Experiments 1–3 are presented, respectively, in Figs. 6–8. The RMSE and bias values shown in the figures were obtained for the data set presented in each figure.

The measured volatilization curves for the three experiments differ in their temporal patterns and in their magnitudes (Figs. 6–8). The highest flux rates in all experiments were recorded just after diazinon application, but the magnitudes of those initial rates differed according to the soil moisture content, with wetter soil producing a higher rate: 5.6×10^{-4} μg cm^{-2} min^{-1} for initial soil moisture above field capacity (Experiment 3), 8.3×10^{-5} μg cm^{-2} min^{-1} for initial soil moisture at field capacity (Experiment 1), and 2.5×10^{-5} μg cm^{-2} min^{-1} for initially very dry soil (Experiment 2). Volatilization decreased during the first day in the two experiments with initially wet soils (Experiments 1 and 3), but remained relatively constant in the experiment with initially dry soil (Experiment 2). The volatilization rate during the first night for the wettest soil (Experiment 3) remained about an order-of-magnitude higher than that observed for driest soil (Experiment 2). When the surface dried in the experiment conducted at the intermediate water content (Experiment 1), the volatilization rate and temporal pattern transitioned and became similar to that

Table 3
Goodness-of-fit measures for the soil temperature.

	Z = 1.5 cm						Z = 5 cm					
	RMSE (°C)	Bias (°C)	NRMSE (%)	$y = ax + b$			RMSE (°C)	Bias (°C)	NRMSE (%)	$y = ax + b$		
				a	B	R^2				a	b	R^2
	Experiment 1: $0.22 \le \theta_w \le 0.048$											
Observations	Average − 31.1 °C, Std − 8.6 °C, n = 59						Average − 30.1 °C, Std − 5.3 °C, n = 59					
BC–D	1.9	−1.0	6	0.90	2.20	0.97	1.2	−0.4	4	1.09	−3.22	0.97
BC–VDG	1.4	−0.17	4	1.01	−0.54	0.98	1.7	0.3	6	1.24	−7.04	0.98
SG–D	2.1	−0.02	7	0.84	4.87	0.95	1.4	0.5	5	1.01	0.31	0.95
SG–VDG	2.9	1.75	9	0.91	4.48	0.93	2.7	2.0	9	1.10	−1.00	0.92
	Experiment 2: $\theta_w \le 0.075$											
Observations	Average − 31.3 °C, Std − 8.4 °C, n = 60						Average − 30.5 °C, Std − 6 °C, n = 60					
BC–D	3	1.7	10	1.25	−6.17	0.98	2.9	1.9	9	1.33	−8.11	0.99
BC–VDG	3.6	2.1	12	1.32	−8.02	0.99	3.4	2.2	11	1.40	−10.10	0.99
SG–D	2.9	1.6	9	1.23	−5.72	0.98	2.7	1.7	9	1.29	−7.24	0.98
SG–VDG	2.4	0.9	8	1.22	−5.97	0.98	2.2	1.1	7	1.27	−7.16	0.98
	Experiment 3: $0.29 \le \theta_w \le 0.13$											
Observations	Average − 28.1 °C, Std − 9.2 °C, n = 60						Average − 27.4 °C, Std − 7.2 °C, n = 60					
BC–D	2	−0.005	7	0.88	3.34	0.96	2.1	0.5	8	0.83	5.08	0.93
BC–VDG	1.6	−0.005	6	0.96	1.05	0.97	1.8	0.41	7	0.91	2.90	0.95
SG–D	2.2	−0.190	8	0.86	3.64	0.95	2.3	0.35	8	0.81	5.49	0.92
SG–VDG	1.7	−0.470	6	0.90	2.14	0.97	1.9	0.07	7	0.85	4.02	0.94

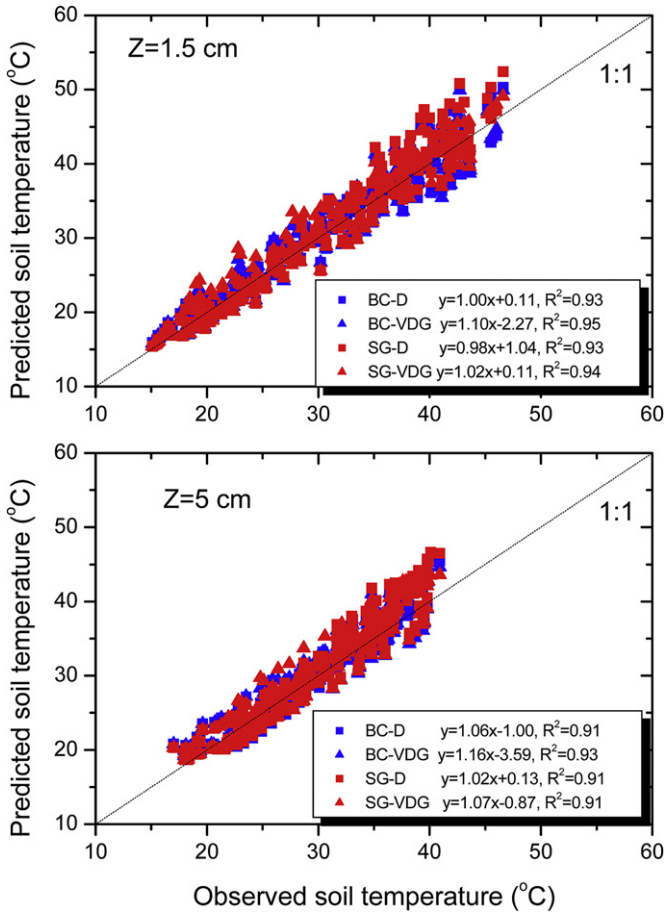

Fig. 3. Scatter plots of observed vs. predicted soil temperatures for experiments 1–3.

observed for the initially dry soil (Experiment 2). Around noon of the second day, a daily maximum value was observed in the volatilization rate for the wet soil (Experiment 3) whereas a minimum value was observed for the dry soils (Experiments 1 and 2), resulting an order-of-magnitude difference.

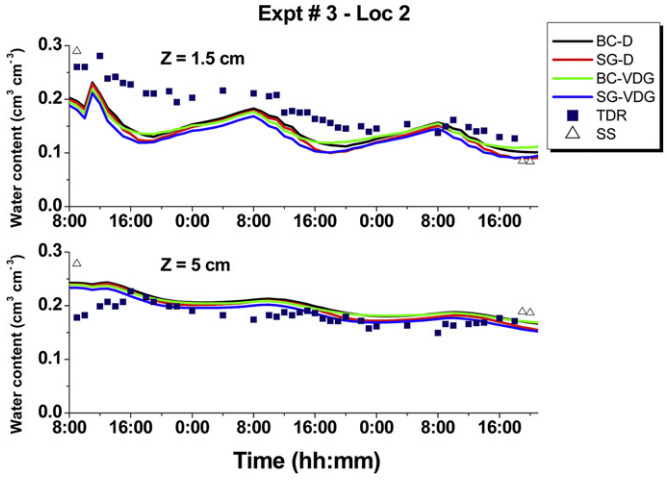

Fig. 4. Temporal variation of measured and simulated soil-water content at two depths (about 1.5 and 5 cm) during the three days of Experiment 3 (Loc 2). (BC = Brooks–Corey water retention function; SG = Silva and Grifoll (2007) full-range water retention model; D = the β wetness surface resistance function of Deardorff (1978); VDG = the surface resistance function proposed by van de Griend and Owe (1994)).

The simulated volatilization curves obtained using the four WR × SSR model configurations differ in their temporal patterns and in their magnitudes (Figs. 6–8). In Experiment 1, the experiment with intermediate water content, the BC–D, BC–VDG and SG–VDG models simulated volatilization curves that generally follow the diurnal variation of the measured curves, while the volatilization in the SG–D model dropped to an almost constant value, lower than observations, about 3 h after application. The four models simulated accurately the volatilization rates during the first hours after application. The BC–D model overestimated observations during the morning and late afternoon hours and underestimated them during the early afternoon hours, while the SG–VDG model underestimated observations during the morning and late afternoon hours and overestimated them during the early afternoon hours. The simulated values obtained with the BC–VDG model closely followed the diurnal variation of observations but overestimated them (Fig. 6). The RMSE and bias values, respectively, were 0.99 and −0.48 for the BC–D model, 0.78 and 0.68 for the BC–VDG model, 1.21 and −1.08 for the SG–D model, and 1.12 and −0.45 for the SG–VDG model (Fig. 6). These results indicate the BC–VDG model predicted the volatilization rates most accurately in experiment 1 with a RMSE of 0.78, which means within a factor of 6 ($=10^{0.78}$).

In Experiment 2, the experiment with the driest soil, the BC–D, SG–D and SG–VDG models overestimated observations during the late afternoon and through the night and early morning hours, and then underestimated them during the late morning and through noon and the early afternoon. The results for the models differ in the magnitude of the deviation between predicted and observed values. Similarly to Experiment 1, the simulated values obtained with BC–VDG model closely followed the diurnal variation of the data but overestimated them (Fig. 7). The RMSE and bias values, respectively, were 0.95 and 0.1 for BC–D model, 1.15 and 1.11 for BC–VDG model, 0.73 and 0.27 for SG–D model, and 0.76 and −0.05 for SG–VDG model (Fig. 7). These results suggests that SG–D and SG–VDG models most accurately predict the volatilization rates in Experiment 2 with RMSE of 0.73 and 0.78, respectively, or within a factor 5.5 and 6, respectively.

In Experiment 3, the experiment with the wettest soil, the four tested models resulted in similar volatilization curves that mainly differed in the magnitude of deviation between the predicted and observed values. The simulated values underestimated observation during the first day and the early afternoon of the next days. An overestimation was observed during late afternoon of the second day, the second night and the morning hours of third day (Fig. 8). The RMSE and bias values, respectively, were 0.9 and −0.28 for the BC–D model, 0.63 and 0.04 for the BC–VDG model, 0.8 and −0.35 for the SG–D model, and 0.82 and −0.41 for the SG–VDG model (Fig. 7). These results suggest the BC–VDG model most accurately predicted the volatilization rates in Experiment 3 with a RMSE of 0.63, or within a factor of 4.

Since the relationships between simulated and observed values are time dependent, each data set was divided into days (e.g. day 1, day 2 and day 3). Each day was further divided into two periods; “14:00–21:00” which covered the hours of afternoon and early evening and “other” which covered the hours of late evening through night, morning and noon. The first period appears just after the solar radiation peak and during this period the soil surface is expected to be very warm and dry. During most of the second period there is no or low solar radiation and the soil surface moisture increased due to condensation (a result of high RH and low surface temperatures), or by upward transport of water vapor from the deeper soil, or by a combination of both mechanisms. A summary of the RMSE and bias values obtained for the different periods is given in Table 5.

Table 4
Goodness-of-fit measures for the soil-water content.

	$Z = 1.5$ cm						$Z = 5$ cm					
	RMSE	Bias	NRMSE	$y = ax + b$			RMSE	Bias	NRMSE	$y = ax + b$		
	($cm^3\ cm^{-3}$)	($cm^3\ cm^{-3}$)	(%)	a	b	R^2	($cm^3\ cm^{-3}$)	($cm^3\ cm^{-3}$)	(%)	a	b	R^2
	Experiment 1											
Observations	Average − 0.114 $cm^3\ cm^{-3}$, Std − 0.053 $cm^3\ cm^{-3}$, $n = 25$						Average − 0.195 $cm^3\ cm^{-3}$, Std − 0.014 $cm^3\ cm^{-3}$, $n = 25$					
BC−D	0.025	−0.002	22	0.59	0.05	0.87	0.021	−0.005	11	1.2	−0.05	0.43
BC−VDG	0.033	0.005	29	0.43	0.07	0.81	0.018	−0.004	9	1.1	−0.02	0.44
SG−D	0.030	−0.018	27	0.69	0.02	0.81	0.035	−0.019	18	1.7	−0.16	0.43
SG−VDG	0.033	−0.019	29	0.61	0.03	0.79	0.034	−0.021	18	1.6	−0.14	0.44
	Experiment 2											
Observations							Average − 0.198 $cm^3\ cm^{-3}$, Std − 0.013 $cm^3\ cm^{-3}$, $n = 52$					
BC−D							0.021	0.005	11	1.3	−0.05	0.42
BC−VDG							0.018	−0.008	9	1.2	−0.03	0.43
SG−D							0.035	0.001	9	1.2	−0.05	0.48
SG−VDG							0.034	−0.013	10	1.1	−0.04	0.48
	Experiment 3											
Observations	Average − 0.184 $cm^3\ cm^{-3}$, Std − 0.041 $cm^3\ cm^{-3}$, $n = 37$						Average − 0.182 $cm^3\ cm^{-3}$, Std − 0.017 $cm^3\ cm^{-3}$, $n = 37$					
BC−D	0.047	−0.041	26	0.66	0.02	0.74	0.026	0.022	15	0.64	0.09	0.27
BC−VDG	0.050	−0.043	27	0.55	0.03	0.77	0.024	0.019	13	0.60	0.10	0.26
SG−D	0.054	−0.048	29	0.72	0.004	0.73	0.023	0.017	13	0.68	0.08	0.26
SG−VDG	0.062	−0.056	33	0.61	0.01	0.74	0.018	0.010	10	0.64	0.08	0.25

The soil moisture of the upper soil layer in Experiments 1 and 3 decreased each day (Table 5). The volumetric threshold (VT) is the water content value below which diazinon volatilization drops off exponentially because of diazinon sorption on the dry soil surfaces. For Experiments 1, 2 and 3, the VT was 0.123, 0.126 and 0.129, respectively (Reichman et al., 2011). Thus, for Experiment 1, the soil-water content in the top 1 cm of soil was above the VT value on the first day (Day 1), around the VT value on the second day (Day 2), and below the VT value on the third day (Day 3). The soil-water content in the top 1 cm of soil was below the VT value throughout Experiment 2, and was above the VT value during Experiment 3 (Table 5).

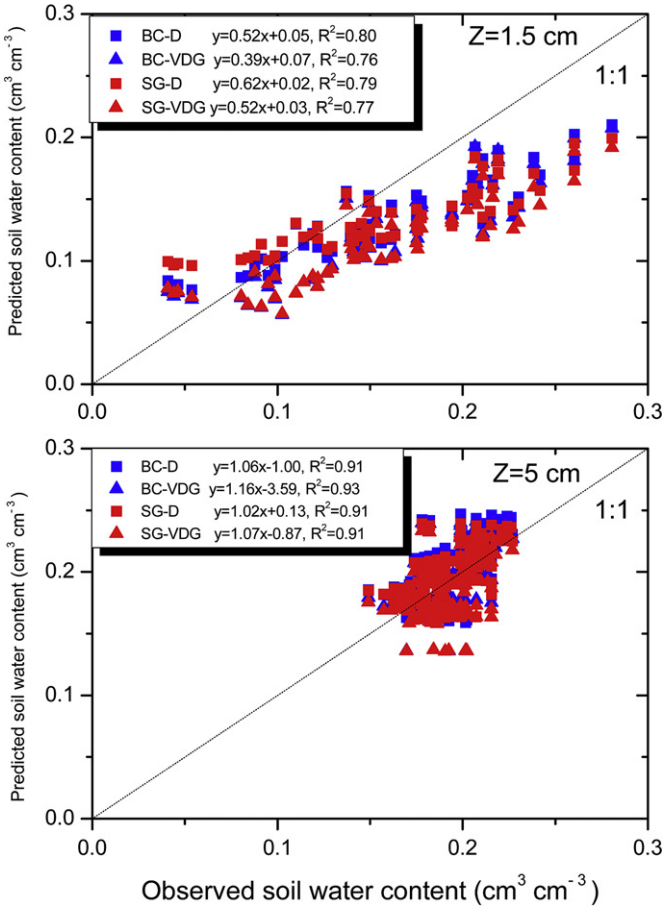

Fig. 5. Scatter plots of observed vs. simulated soil-water content for experiments 1–3.

For the first two days of Experiment 1, when the soil-water content in the top 1 cm of soil was above or around the VT, volatilization rates predicted with the BC−VDG model were the most accurate for both of the daily time periods ("14:00–21:00", "other"), although the accuracy was lower on the second day; on the first day RMSE values were 0.4 and 0.44, whereas on the second they were 0.74 and 0.78. On the third day, when the soil-water content in the top 1 cm of soil was below the VT, the SG−D model predictions were the most accurate with an average RMSE value of 0.6.

During the three days of Experiment 2 the soil-water content in the top 1 cm of soil was below the VT value and the SG−D and SG−VDG models were the most accurate. Lower values of RMSE and bias were obtained during the "other" hours when soil moisture increased (Table 5). In Experiment 3, the model that had the lowest RMSE values (best accuracy) varied through the six identified time periods. On the first day, the models with the lowest RMSE values for the dry period (14:00–21:00) and moist period ("other") were BC−D and BC−VDG, respectively. The emissions in the dry and moist periods, respectively, were best predicted for the second day using the SG−D and BC−VDG models, and for the third day using SG−VDG and BC−VDG models (Table 5).

The results indicate that under severe dry conditions, when soil-water content in the top 1 cm is below the volumetric threshold value, the use of full-range WR function (SG) proposed by Silva and Grifoll (2007) resulted in the most accurate prediction of pesticide emission rates. Otherwise, the Brooks–Corey (BC) function was found to be adequate (recall that the SG and BC water retention models are identical for matric pressures above -1.5×10^4 cm). For simulating pesticide emission under normal practice conditions where initial soil moisture is about field capacity (e.g. Experiment 1) or higher (e.g. Experiment 3), the BC−VDG model should be sufficient. The effect of the SSR function on the prediction accuracy depends on the WR function used and the soil moisture. Under wet conditions (Experiments 1 and 3), the BC function used in conjunction with the VDG function resulted in more accurate predictions (Figs. 6and 8), while in dry conditions (Experiment 2)

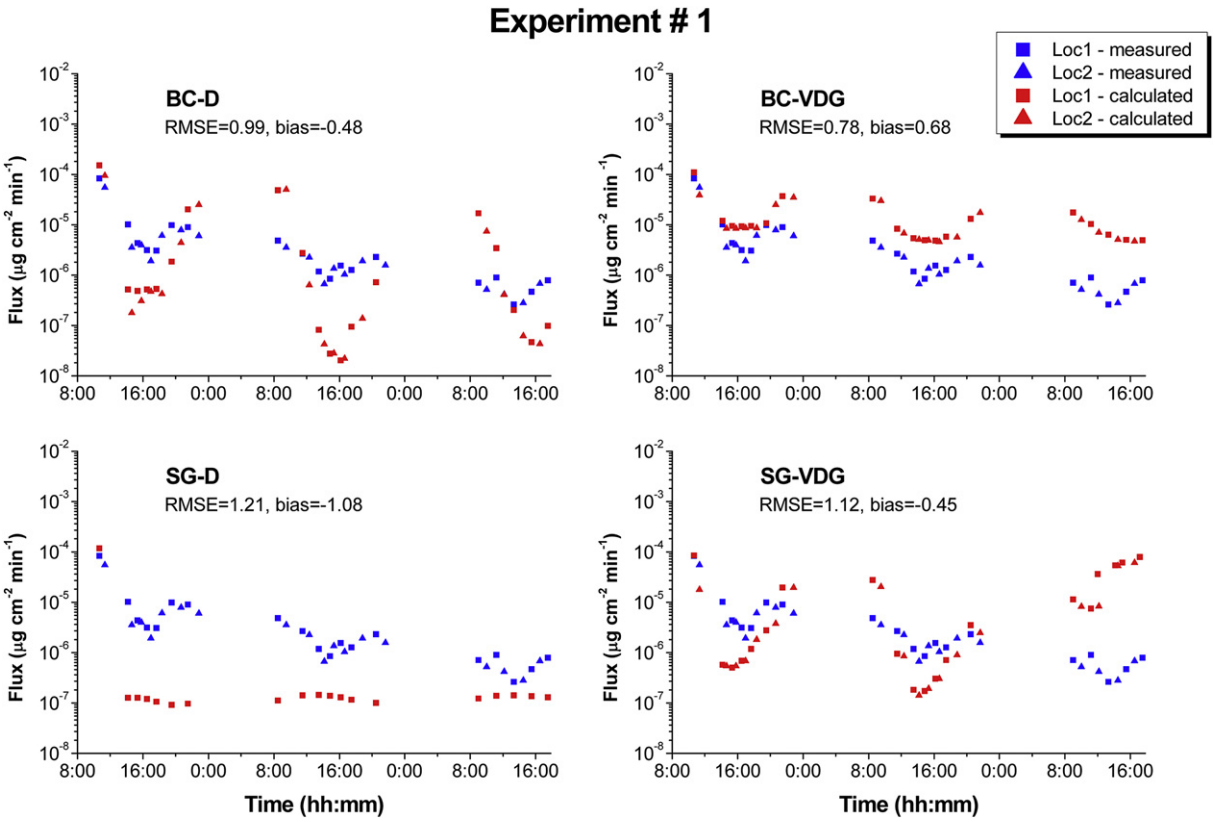

Fig. 6. Temporal variation of measured and predicted fluxes for the three days of Experiment 1. (BC = Brooks–Corey water retention function; SG = Silva and Grifoll (2007) full-range water retention model; D = the β wetness surface resistance function of Deardorff (1978); VDG = the surface resistance function proposed by van de Griend and Owe (1994)).

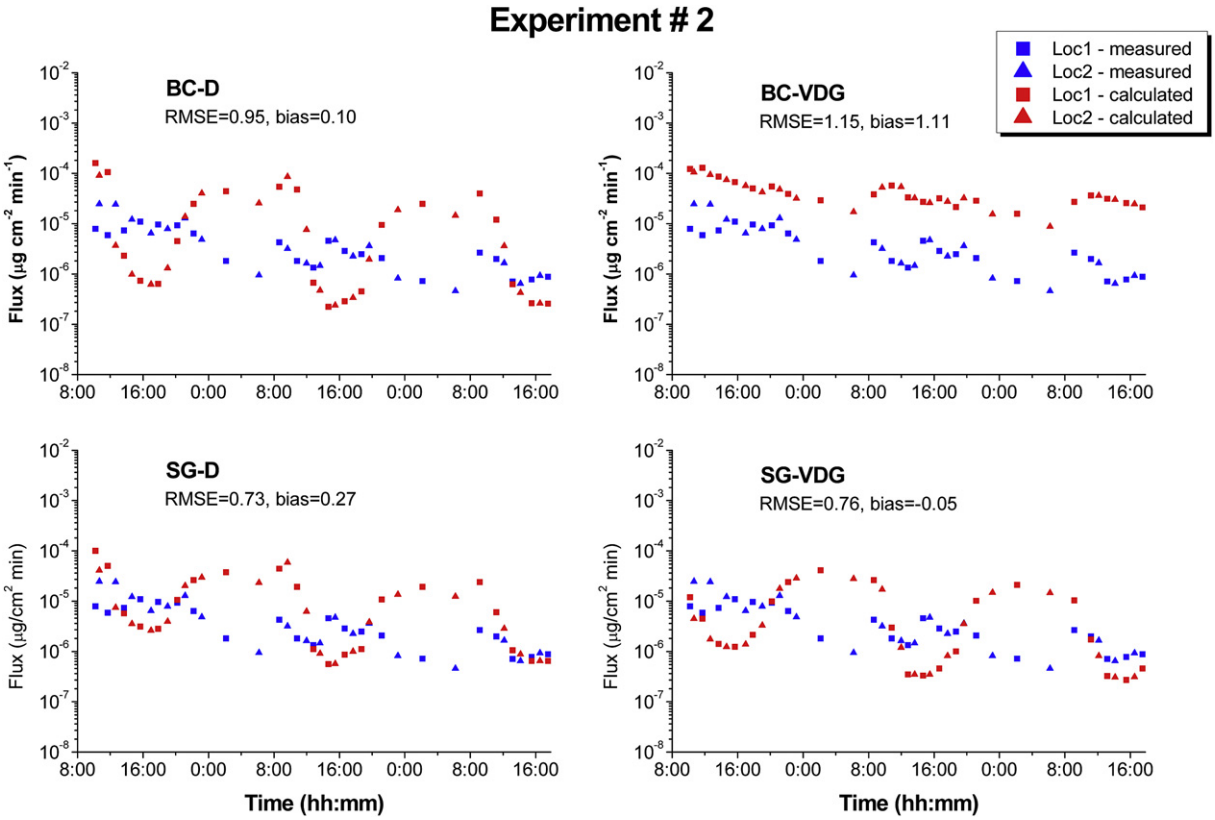

Fig. 7. Temporal variation of measred and simulated fluxes for the three days of Experiment 2. (BC = Brooks–Corey water retention function; SG = Silva and Grifoll (2007) full-range water retention model; D = the β wetness surface resistance function of Deardorff (1978); VDG = the surface resistance function proposed by van de Griend and Owe (1994)).

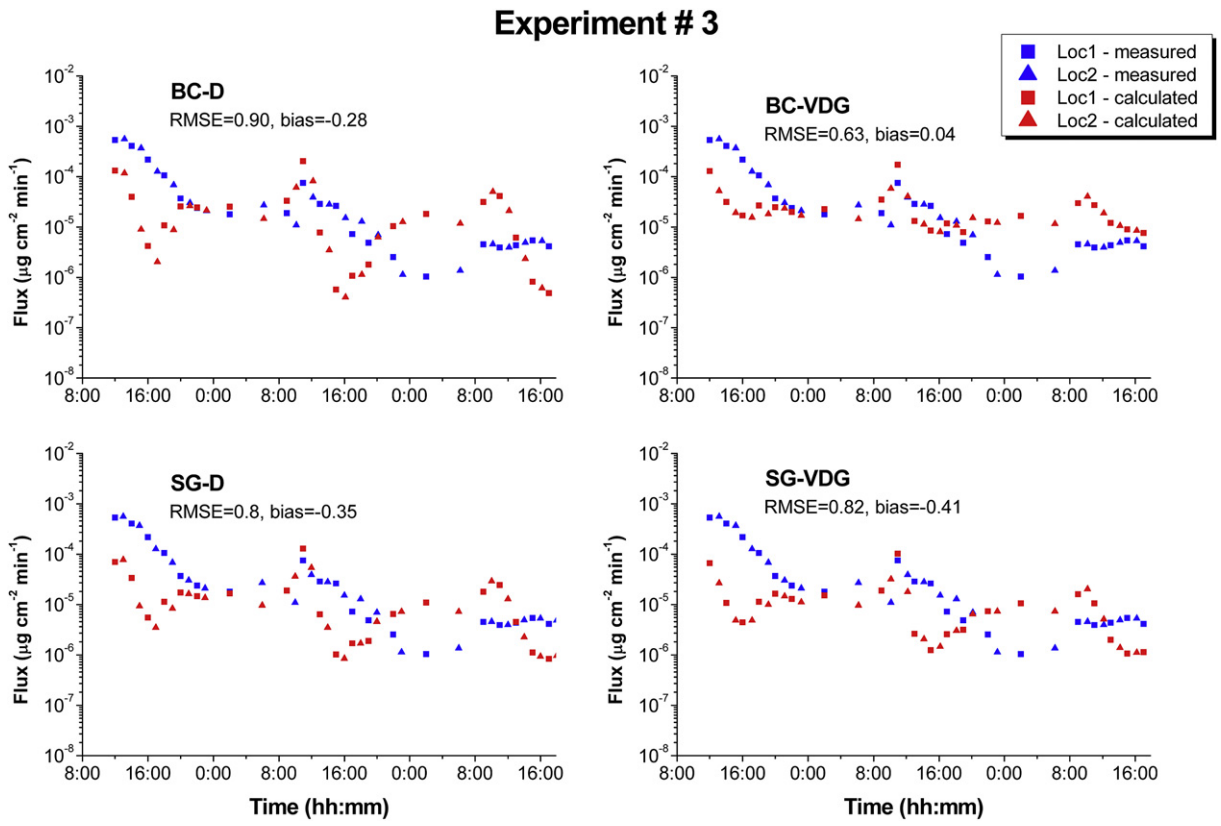

Fig. 8. Temporal variation of measured and simulated fluxes for the three days of Experiment 3. (BC = Brooks–Corey water retention function; SG = Silva and Grifoll (2007) full-range water retention model; D = the β wetness surface resistance function of Deardorff (1978); VDG = the surface resistance function proposed by van de Griend and Owe (1994)).

the BC–D combination was more accurate (Fig. 7). The SSR function had a minor effect when used with the SG retention function (Figs. 6–8).

3.4. Flux chamber effect

The flux chamber has the potential to influence the environmental conditions at the soil surface, which could affect the measured flux rate. This was tested by performing additional simulations without a chamber and comparing the results with measured data and simulations made with a chamber. The test was performed for conditions that existed in Experiment 3 using the BC–VDG model.

Chamber effects on the diurnal variation soil temperature and volatilization rates are presented in Figs. 9and 10, respectively. The presence of the flux chamber did not affect the soil-water content

Table 5
Goodness-of-fit measures for the volatilization fluxes in each experiment.

Model	Day 1		Day 2		Day 3	
	14:00–21:00	Other	14:00–21:00	Other	14:00–21:00	Other
	RMSE (bias)	RMSE (bias)	RMSE (bias)	RMSE (bias)	RMSE (bias)	RMSE (bias)
	Experiment 1					
	θ_w: 0.22–0.11[a]		θ_w: 0.11–0.10		θ_w: 0.10–0.048	
BC–D	0.74 (−0.04)	0.86 (−0.73)	0.95 (−0.13)	1.35 (−1.10)	0.85 (0.60)	0.88 (−0.85)
BC–VDG	0.40 (0.20)	0.44 (0.40)	0.74 (0.71)	0.70 (0.68)	1.30 (1.29)	1.00 (0.99)
SG–D	1.31 (−0.85)	1.64 (−1.62)	1.23 (−1.19)	1.08 (−1.07)	0.61 (−0.58)	0.60 (−0.57)
SG–VDG	1.04 (−0.83)	1.17 (−0.98)	0.96 (−0.65)	0.85 (−0.72)	1.27 (0.65)	1.41 (0.46)
	Experiment 2					
	$\theta_w \leq 0.075$[b]		$\theta_w \leq 0.075$		$\theta_w \leq 0.075$	
BC–D	0.90 (0.47)	0.91 (−0.79)	1.15 (0.89)	0.94 (−0.68)	0.98 (0.73)	0.47 (−0.04)
BC-VDG	0.96 (0.92)	0.76 (0.76)	1.31 (1.30)	0.97 (0.96)	1.38 (1.36)	1.46 (0.20)
SG–D	0.70 (0.43)	0.41 (−0.30)	1.01 (0.84)	0.62 (−0.33)	0.87 (0.69)	0.15 (−0.85)
SG–VDG	0.69 (−0.17)	0.65 (−0.50)	0.92 (0.50)	0.76 (−0.46)	0.85 (0.36)	0.37 (−0.83)
	Experiment 3					
	θ_w: 0.26–0.21[a]		θ_w: 0.21–0.14		θ_w: 0.14–0.13	
BC–D	0.46 (−0.31)	1.20 (−1.03)	0.56 (0.30)	1.07 (−0.93)	0.91 (−0.85)	0.82 (−0.79)
BC–VDG	0.60 (−0.45)	0.84 (−0.73)	0.53 (0.29)	0.31 (−0.07)	0.86 (−0.84)	0.25 (0.24)
SG–D	0.63 (−0.54)	1.16 (−1.04)	0.45 (0.11)	0.91 (−0.81)	0.71 (−0.64)	0.65 (−0.64)
SG–VDG	0.82 (−0.69)	1.26 (−1.13)	0.53 (−0.003)	0.82 (−0.68)	0.61 (−0.45)	0.61 (−0.60)

[a] Based on TDR measurements at $z = 1.5$ cm.
[b] Based on 0–2 cm soil sampling and gravimetric determination.

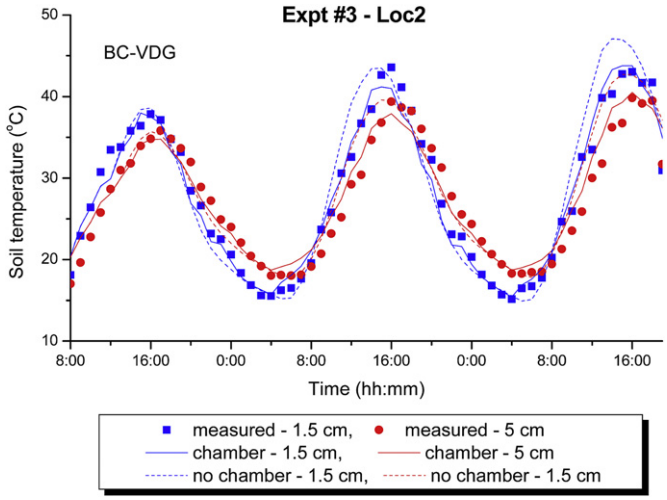

Fig. 9. Flux chamber effect on soil temperature for conditions existing in Experiment 3 using the BC-VDG model, (BC = Brooks–Corey water retention function; VDG = the surface resistance function proposed by van de Griend and Owe (1994)). The notation "chamber" and "no chamber" refer to simulated values resulted in considering and ignoring the presence of the chamber, respectively.

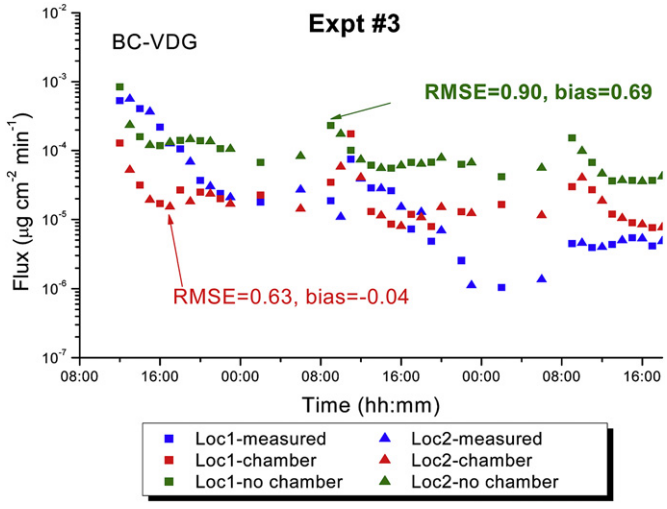

Fig. 10. Flux chamber effect on volatilization fluxes for conditions existing in Experiment 3 using the BC-VDG model, (BC = Brooks–Corey water retention function; VDG = the surface resistance function proposed by van de Griend and Owe (1994)). The notation "chamber" and "no chamber" refer to simulated values resulted in considering and ignoring the presence of the chamber, respectively.

(data not presented). The chamber had a minor effect on soil temperature and volatilization rates. Simulations without the chamber produced earlier daily soil temperature peaks on days 2 and 3, and higher values on day 3 (Fig. 9). The RMSE, bias, and NRMSE values for simulations without the chamber were 2.8 °C, 0.93 °C, and 10.2% respectively. These values were slightly higher than the values obtained when the chamber was included (1.8 °C, 0.41 °C, and 6.6%). In general, simulations without the chamber resulted in higher volatilization rates (Fig. 10). The RMSE and bias values were also higher, being, respectively, 0.90 and −0.69 without the chamber vs. 0.63 and 0.04 with the chamber. Still, the RMSE and bias values for the BC–VDG model and no chamber were within the range of values obtained for the other three models when the chamber was included (Fig. 8). Placing the chamber for longer periods of time will probably increase the underestimation of the evaluated flux due to further decrease of soil surface temperature.

4. Conclusions

Water retention (WR) and soil surface resistance (SSR) functions strongly affect the volatilization pattern. The degree of similarity between the volatilization curves simulated by the four models depended on the initial water content. Under fairly wet conditions (e.g. Experiment 3) the four tested models resulted in similar volatilization curves that mainly differed in the magnitude of their deviation from the measured values. However, under intermediate (e.g. Experiment 1) and low (e.g. Experiment 2) moisture conditions, the simulated volatilization curves differed in their temporal pattern, as well. Similar results were reported by Reichman et al. (submitted for publication) based on a numerical sensitivity analysis preformed for a loam soil. The accuracy of model predictions depended on model type and soil moisture. Under normal diazinon application conditions, where initial soil moisture was about field capacity (e.g. Experiment 1) or higher (e.g. Experiment 3), using the BC–VDG model resulted in the most accurate prediction of pesticide emission. However, under extremely dry conditions, when soil-water content in the top 1 cm was below the volumetric threshold value, the use of full-range WR function increased the accuracy of the predicted diazinon emission rates. The simulating volatilization rates had a RMSE value of 0.64, i.e. were accurate to within a factor of 4 ($10^{0.64}$).

Soil temperature predictions were not affected by the WR and SSR functions. The SSR function had a minor effect on the predicted soil-water content of Yolo silty clay soil, but a greater effect was simulated for sand (Reichman et al., submitted for publication). The flux chamber had a minor effect on environmental conditions and volatilization rates when used for 30–60 min sampling.

References

Avissar, R., Mahrer, Y., 1982. Verification study of a numerical greenhouse microclimate model. Trans. ASAE 25, 1711–1720.
Baker, J.M., Koskinen, W.C., Dowdy, R.H., 1996. Volatilization of EPTC: simulation and measurement. J. Environ. Qual. 25, 169–177. doi:10.2134/jeq1996.00472425002500010022x.
Bedos, C., Genermont, S., le Cadre, E., Garcia, L., Barriuso, E., Cellier, P., 2009. Modeling pesticide volatilization after soil application using the mechanistic model volt'air. Atmos. Environ. 43, 3630–3639. doi:10.1016/j.atmosenv.2009.03.024.
Brooks, R.H., Corey, A.T.C., 1964. Hydraulic Properties of Porous Media. Hydrol. Pap. 3. Colo. State Univ., Fort Collins.
Bro-Rasmussen, F., Nbddegaard, E., Voldum-Clausen, K., 1970. Comparison of the disappearance of eight organophosphorus insecticides from soil in laboratory and in outdoor experiments. Patic. Sci. 1, 179–182.
Chen, D., Rolston, D.E., Yamaguchi, T., 2000. Calculating partition coefficients of organic vapors in unsaturated soil and clays. Soil Sci. 165, 217–225.
Deardorff, J.W., 1978. Efficient prediction of ground surface temperature and moisture, with inclusion of a layer of vegetation. J. Geophys. Res. 83, 1889–1903.
Fuller, E.N., Schettler, P.D., Giddings, J.C., 1966. A new method for prediction of binary gas-phase diffusion coefficient. Ind. Eng. Chem. 58, 19–27.
Gish, T.J., Prueger, J.H., Kustas, W.P., Daughtry, C.S.T., McKee, L.G., Russ, A., Hatfield, J.L., 2009. Soil moisture and metolachlor volatilization observations over three years. J. Environ. Qual. 38, 1785–1795. doi:10.2134/jeq2008.0276.
Glotfelty, D.E., Leech, M.M., Jersey, J., Taylor, A.W., 1989. Volatilization and wind erosion of soil surface applied atrazine, simazine, alachlor, and toxaphene. J. Agric. Food Chem. 37, 546–551.
Glotfelty, D.E., Taylor, A.W., Turner, B.C., Zoller, W.H., 1984. Volatilization of surface-applied pesticides from fallow soil. J. Agric. Food Chem. 32, 638–643.
Gong, Y., Cao, Q., Sun, Z., 2003. The effects of soil bulk density, clay content and temperature on soil water content measurement using time-domain reflectometry. Hydrol. Process 17, 3601–3614.
Kim, Y., Woodrow, J.W., Seiber, J.N., 1984. Evaluation of a gas chromatographic method calculating vapor pressures with organophosphorus pesticides. J. Chromatogr. 314, 37–53.
Kimball, B.A., 1973. Simulation of the energy balance of a greenhouse. Agric. Meteorol. 11, 243–260.
Lin, S.Y., Lin, L.W., Chang, H.C., Ku, Y., 1996. Adsorption kinetics of diazinon at the air–water interface. J. Phys. Chem. 100, 16678–16684.
Prueger, J.H., Gish, T.J., McConnell, L.L., Mckee, L.G., Hatfield, J.L., Kustas, W.P., 2005. Solar radiation, relative humidity, and soil water effects on metolachlor volatilization. Environ. Sci. Technol. 39, 5219–5226. doi:10.1021/es048341q.

Reichman, R., Rolston, D.E., Yates, S.R., Skaggs, T.H., 2011. Diurnal variation of diazinon volatilization: soil moisture effects. Environ. Sci. Technol. 45 (6), 2144–2149. doi:10.1021/es102921r.

Reichman, R., Yates, S.R., Skaggs, T.H., submitted for publication. Numerical study on the effect of soil moisture on the diurnal pattern of pesticide emission. Atmos. Environ.

Reichman, R., Rolston, D.E., 2002. Design and performance of a dynamic gas flux chamber. J. Environ. Qual. 31, 1774–1781. doi:10.2134/jeq2002.1774.

Reichman, R., Wallach, R., Mahrer, Y., 2000. A combined soil-atmosphere model for evaluating the fate of surface-applied volatile organic chemicals. 1. Model development and verification. Environ. Sci. Technol. 34 (7), 1313–1320. doi:10.1021/es990356e.

Reif, R., 1976. Fundamentals of Statistical and Thermal Physics. McGraw-Hill, Inc., Boston MS.

Scholtz, M.T., Voldner, E., McMillan, A.C., Van Heyst, B.J., 2002a. A pesticide emission model (PEM) part I: model development. Atmos. Environ. 36, 5005–5013. doi:10.1016/S1352-2310(02)00570-8.

Scholtz, M.T., Voldner, E., Van Heyst, B.J., McMillan, A.C., Pattey, E., 2002b. A pesticide emission model (PEM) part II: model evaluation. Atmos. Environ. 36, 5015–5024. doi:10.1016/S1352-2310(02)00571-X.

Silva, O., Grifoll, J., 2007. A soil-water retention function that includes the hyper-dry region through the BET adsorption isotherm. Water Resour. Res. 43, W11420. doi:10.1029/2006WR005325.

Spencer, W.F., Cliath, M.M., 1973. Pesticide volatilization as related to water loss from soil. J. Environ. Qual. 2, 284–289.

Spencer, W.F., Cliath, M.M., Farmer, W.J., 1969. Vapor density of soil-applied dieldrin as related to soil-water content, temperature, and dieldrin concentration. Soil Sci. Soc. Am. Proc. 33, 509–511.

Spencer, W.F., Farmer, W.J., Jury, W.A., 1982. Review: behavior of organic chemicals at soil, air, water interfaces as related to predicting the transport and volatilization of organic pollutants. Environ. Toxicol. Chem. 1, 17–26.

Taylor, A.W., Spencer, W.F., 1990. Volatilization and vapor transport processes. In: Pesticides in the Soil Environment: Processes, Impacts and Modeling. Soil Science Society of America Book Series, No. 2. SSSA, Madison, WI, Chapter 7, pp 213–269.

van de Griend, A., Owe, M., 1994. Bare soil surface resistance to evaporation by vapor diffusion under semiarid conditions. Water Resour. Res. 30 (2), 181–188.

Wang, D., Yates, S.R., Jury, W.A., 1998. Temperature effect on methyl bromide volatilization: permeability of plastic cover films. J. Environ. Qual. 27, 821–827. doi:10.2134/jeq1998.00472425002700040015x.

Wang, D., Yates, S.R., Gan, J., 1997. Temperature effect on methyl bromide volatilization in soil fumigation. J. Environ. Qual. 26, 1072–1079. doi:10.2134/jeq1997.00472425002600040019x.

Yates, S.R., 2006. Simulating herbicide volatilization from bare soil affected by atmospheric conditions and limited solubility in water. Environ. Sci. Technol. 40, 6963–6968. doi:10.1021/es061303h.